

Mid- to late Holocene hydroclimatic changes on the Chinese Loess Plateau

Sun, Huiling; Bendle, James; Seki, Osamu; Zhou, Aifeng

DOI:

[10.1007/s10933-018-0037-9](https://doi.org/10.1007/s10933-018-0037-9)

License:

Other (please specify with Rights Statement)

Document Version

Peer reviewed version

Citation for published version (Harvard):

Sun, H, Bendle, J, Seki, O & Zhou, A 2018, 'Mid- to late Holocene hydroclimatic changes on the Chinese Loess Plateau: evidence from n-alkanes from the sediments of Tianchi Lake', *Journal of Paleolimnology*, vol. 60, no. 4, pp. 511-523. <https://doi.org/10.1007/s10933-018-0037-9>

[Link to publication on Research at Birmingham portal](#)

Publisher Rights Statement:

The final publication is available at Springer via <http://doi.org/10.1007/s10933-018-0037-9>

General rights

Unless a licence is specified above, all rights (including copyright and moral rights) in this document are retained by the authors and/or the copyright holders. The express permission of the copyright holder must be obtained for any use of this material other than for purposes permitted by law.

- Users may freely distribute the URL that is used to identify this publication.
- Users may download and/or print one copy of the publication from the University of Birmingham research portal for the purpose of private study or non-commercial research.
- User may use extracts from the document in line with the concept of 'fair dealing' under the Copyright, Designs and Patents Act 1988 (?)
- Users may not further distribute the material nor use it for the purposes of commercial gain.

Where a licence is displayed above, please note the terms and conditions of the licence govern your use of this document.

When citing, please reference the published version.

Take down policy

While the University of Birmingham exercises care and attention in making items available there are rare occasions when an item has been uploaded in error or has been deemed to be commercially or otherwise sensitive.

If you believe that this is the case for this document, please contact UBIRA@lists.bham.ac.uk providing details and we will remove access to the work immediately and investigate.

Journal of Paleolimnology

Mid- to- late Holocene hydroclimatic changes on the Chinese Loess Plateau: evidence from n-alkanes from the sediments of Tianchi Lake --Manuscript Draft--

Manuscript Number:	JOPL-D-17-00035R4	
Full Title:	Mid- to- late Holocene hydroclimatic changes on the Chinese Loess Plateau: evidence from n-alkanes from the sediments of Tianchi Lake	
Article Type:	Papers	
Keywords:	n-Alkanes · Paq · Lake level · Mid-late Holocene · Loess Plateau	
Corresponding Author:	Aifeng Zhou Lanzhou University Lanzhou, Gansu CHINA	
Corresponding Author Secondary Information:		
Corresponding Author's Institution:	Lanzhou University	
Corresponding Author's Secondary Institution:		
First Author:	Huiling Sun	
First Author Secondary Information:		
Order of Authors:	Huiling Sun	
	James Bendle	
	Osamu Seki	
	Aifeng Zhou	
Order of Authors Secondary Information:		
Funding Information:	National Natural Science Foundation of China (41761044)	Dr. Huiling Sun
	National Natural Science Foundation of China (41771208)	Dr. Aifeng Zhou
	China Scholarship Council (2009618032)	Dr. Huiling Sun
Abstract:	<p>We have reconstructed the history of mid-late Holocene paleohydrological changes in the Chinese Loess Plateau using n-alkane data from a sediment core in Tianchi Lake. We used Paq (the proportion of aquatic macrophytes to the total plant community) to reflect changes in lake water level, with a higher abundance of submerged macrophytes indicating a lower water level and vice versa. The Paq -based hydrological reconstruction agrees with various other lines of evidence, including ACL (average chain length), CPI (carbon preference index), C/N ratio and the n-alkane molecular distribution of the sediments in Tianchi Lake. The results reveal that the lake water level was relatively high during 5.7 to 3.2 ka BP, and decreased gradually thereafter. Our paleohydrological reconstruction is consistent with existing paleoclimate reconstructions from the Loess Plateau, which suggest a humid mid-Holocene, but is asynchronous with paleoclimatic records from central China which indicate an arid mid-Holocene. Overall, our results confirm that the intensity of the rainfall delivered by the EASM (East Asian summer monsoon) is an important factor in affecting paleohydrological changes in the region and can be considered as further evidence for the development of a spatially asynchronous "northern China drought and southern China flood" precipitation pattern during the Holocene.</p>	
Suggested Reviewers:	Cheng Zhao Professor, Nanjing Institute of Geography and Limnology Chinese Academy of	

	Sciences czhao@niglas.ac.cn
	Zhonghui Liu Professor, University of Hong Kong zhliu@hku.hk
	James Russell associate professor, Brown University James_Russell@brown.edu
Response to Reviewers:	<p>Dear Professor Whitmore,</p> <p>Thanks you so much for your corrected my manuscript. I accepted all the corrections and “accept all changes”.</p> <p>Best regards!</p> <p>Sincerely,</p> <p>Aifeng</p>

[Click here to view linked References](#)

Mid- to- late Holocene hydroclimatic changes on the Chinese Loess

Plateau: evidence from *n*-alkanes from the sediments of Tianchi Lake

Huiling Sun^a · James Bendle^b · Osamu Seki^c · Aifeng Zhou^{d*}

2

a. *Key Laboratory of Plateau Lake Ecology and Global Change, College of Tourism*

and *Geography, Yunnan Normal University, Kunming, 650500, China*

b. *School of Geography, Earth and Environmental Sciences, University of*

Birmingham, Edgbaston, Birmingham, B15 2TT, UK

c. *Institute of Low Temperature Science, Hokkaido University, N19W8, Kita-ku,*

Sapporo, 060-0819, Japan

d. *Key Laboratory of Western China's Environmental Systems (Ministry of Education),*

College of Earth and Environmental Sciences, Lanzhou University, Lanzhou, 730000,

China

12

* Corresponding Author: Aifeng Zhou (zhouaf@lzu.edu.cn)

Address: 222 Tianshui South Road, Lanzhou, Gansu, P.R.China. 730000

Phone: (+86)13893612602

16

Key words

n-Alkanes · P_{aq} · Lake level · Mid-late Holocene · Loess Plateau

19

Abstract

We have reconstructed the history of mid-late Holocene paleohydrological changes in the Chinese Loess Plateau using *n*-alkane data from a sediment core in Tianchi Lake. We used P_{aq} (the proportion of aquatic macrophytes to the total plant community) to reflect changes in lake water level, with a higher abundance of submerged macrophytes indicating a lower water level and vice versa. The P_{aq} -based hydrological reconstruction agrees with various other lines of evidence, including ACL (average chain length), CPI (carbon preference index), C/N ratio and the *n*-alkane molecular distribution of the sediments in Tianchi Lake. The results reveal that the lake water level was relatively high during 5.7 to 3.2 ka BP, and decreased gradually thereafter. Our paleohydrological reconstruction is consistent with existing paleoclimate reconstructions from the Loess Plateau, which suggest a humid mid-Holocene, but is asynchronous with paleoclimatic records from central China which indicate an arid mid-Holocene. Overall, our results confirm that the intensity of the rainfall delivered by the EASM (East Asian summer monsoon) is an important factor in affecting paleohydrological changes in the region and can be considered as further evidence for the development of a spatially asynchronous “northern China drought and southern China flood” precipitation pattern during the Holocene.

Introduction

Climatic and environmental changes in the Chinese Loess Plateau are mainly controlled by the EASM, which directly affects almost all aspects of the hydrology and ecology of East Asia (Clift and Plumb 2008). An increase in EASM intensity would be expected to result in a northward movement of the rainfall belt in China and a corresponding rainfall increase in the Loess Plateau (Chen et al. 2008). Many regional paleoclimatic records have been produced from this semi-arid, monsoon marginal zone (Zhao et al. 2010; Dong et al. 2012; Liu and Feng 2012; Lu et al. 2013; Qiang et al. 2013). However, regional high-resolution paleohydrological reconstructions are extremely limited because proxies or archives that record ancient hydrological conditions, with good age control, are scarce on the Loess Plateau. A humid mid-Holocene has been proposed based on a pollen-based record (Chen et al. 2015a) and a hydrogen isotope reconstruction of long-chain *n*-alkanes (Rao et al. 2016) from Gonghai Lake, one of the few natural lakes on the Loess Plateau. Their paleohydrological reconstruction is inconsistent with records from the core monsoon-controlled regions of central China. It shows an arid interval from 7.0-3.0 ka BP (Xie et al. 2013; Zhu et al. 2017). Therefore, more high-resolution lacustrine reconstructions of hydroclimatic variations during the mid-late Holocene are needed to explore the underlying mechanism of this asynchronous hydroclimatic variability. Here, a high-resolution lacustrine record based on *n*-alkanes of sediments from Tianchi Lake on the Loess Plateau will be discussed.

1 64 *n*-Alkanes preserved in lake sediments can be used to infer variations in the
2
3 65 composition and origin of organic inputs to the lacustrine environment, because they
4
5 66 are widely preserved in various environmental contexts, such as plants, soils and
6
7
8 67 lacustrine sediments, and can resist degradation actions (Meyers 1997). In particular
9
10
11 68 the Average Chain Length (ACL) (Poynter and Eglinton 1990), Carbon Preference
12
13
14 69 Index (CPI) (Meyers and Ishiwatari 1993), and P_{aq} (Ficken et al. 2000) *n*-alkane
15
16
17 70 indices, have been widely used in paleoenvironmental research (Nichols et al. 2006;
18
19
20 71 He et al. 2014). In general, terrestrial plants and emergent macrophytes are typically
21
22
23 72 dominated by the long-chain length homologues (C_{27} - C_{33}) (Ficken et al. 2000; Gao et
24
25
26 73 al. 2011), while submerged and floating-leaved macrophytes mainly produce C_{23} and
27
28
29 74 C_{25} *n*-alkanes (Ficken et al. 2000), and short chain ones are produced by algae and
30
31
32 75 bacteria (Cranwell et al. 1987). Consequently, higher ACL and CPI are commonly
33
34
35 76 considered to be predominantly produced by terrestrial plants. A higher P_{aq} may result
36
37
38 77 from an increase in submerged macrophytes in combination with a recession of the
39
40
41 78 terrestrial plants around the lake. Moreover, the biomass of submerged macrophytes is
42
43
44 79 related to the variation of the water table (Wagner and Falter 2002; Liu et al. 2015),
45
46
47 80 and lake level fluctuations have the potential to simultaneously constrain the spatial
48
49
50 81 distribution and the biomass of submerged macrophytes in a lake (Duarte and Kalf
51
52
53 82 1986; Hudon 1997; Middelboe and Markager 1997). However, Aichner et al. (2010)
54
55
56 83 and Liu et al. (2015) found that higher amounts of long chain *n*-alkanes can be
57
58
59 84 produced by submerged macrophytes in several lakes. Therefore, it is necessary to
60
61
62 85 understand the extent to which long chain *n*-alkanes in lacustrine sediments are
63
64
65

1 86 influenced by terrestrial plants and submerged macrophytes in a study lake when
2
3 87 reconstructing the paleoenvironments.
4
5

6 88 In this study, we first define the potential sources and the contributions from the
7
8 89 various plants (e.g. terrigenous plants vs. submerged macrophytes) in Tianchi Lake.
9
10
11 90 Second, we give an interpretation of the proxies (P_{aq} , ACL, CPI of *n*-alkanes, and
12
13
14 91 C/N), especially P_{aq} as an effective indicator of lake level changes in Tianchi Lake.
15
16
17 92 Additionally, we seek to compare regional climate reconstructions with those from
18
19
20 93 Tianchi Lake and other nearby sites to confirm a spatially asynchronous
21
22
23 94 hydroclimatic variability occurred in China during the Holocene.
24
25

26 95

27 96 Study site

28
29
30

31 97

32
33
34 98 Tianchi Lake (lat. 35°15'55"N, long. 106°18'43"E, elevation 2430 m a.s.l.) is a small
35
36
37 99 freshwater alpine lake located in the Liupan Mountains, southwestern Loess Plateau,
38
39 100 northwest China (Fig. 1a). The length of the lake from east to west is 250 m and the
40
41
42 101 width is 120 m. The maximum water depth is 8.2 m, and the lake covers an area of
43
44
45 102 2×10^4 m² (Fig. 1b). The lake receives no surface run off, and it is fed by meteoric
46
47
48 103 water and groundwater recharge. There is no apparent surface outflow, except for a
49
50
51 104 possible transient outflow in the western part of the lake basin, which is possibly
52
53
54 105 active during the rainy season. The mean annual temperature is 8.2 °C and mean
55
56
57 106 annual precipitation is 677 mm based on data from the nearest meteorological station
58
59 107 (Liupan Mountain station, at 2845 m a.s.l.). Most of the precipitation occurs as
60
61
62
63
64
65

rainfall during summer, accounting for nearly 72.2% of the annual total. The vegetation of the upland slopes of the lake is dominated by shrubs and steppe. Grassy steppe with sparse shrub covers the north slopes, and shrubs dominate the south slopes (Zhao et al. 2010). Emergent (*Phragmites australis* (Cav.) Trin. ex Steud) and submerged (*Potamogeton* sp. and *Chara* sp.) macrophytes are widely distributed in the shallow areas of the lake (Fig. 1d), but floating-leaved macrophytes are absent, based on our field observations in 2010.

Materials and methods

Field sampling

Two parallel sediment cores of lengths 11.2 m (GSA07-1) and 10.4 m (GSB07-1) were collected using a UWITEC piston corer system (6 cm in diameter) from the lake center in 2007 (Fig. 1b). The lithology of core GSB07-1 consisted of alternating brown-colored sandy clay and grey-brownish clay between 1040-746 cm, and grey-brownish clay above 746 cm. The sediments are characterized by 1 to 2-mm-thick organic detritus-rich laminations (Fig. 1c), which yielded abundant terrestrial macrofossils for radiocarbon dating. Fifty-six down-core sedimentary samples were taken at 15-cm intervals throughout core GSB07-1. Additionally, we collected six surface soil samples, three surface lake sediments, nine dominant terrestrial plant samples (*Cedrus* sp., *Larix* sp., *Abies* sp., *Betula* sp., *Rosa* sp., *Rubus*

sp., *Salix* sp., *Berberis* sp. and *Artemisia* sp.), which surround the lake, and one emergent macrophyte (*P. australis*) and two submerged macrophytes (*Potamogeton* and *Chara*) within the lake for modern process study. All the above samples were carried out for TOC, TN analyses, and lipid extraction.

Laboratory analyses

Samples for TOC and TN measurements were pretreated with 10 ml of 10% HCl to remove carbonates, washed with distilled water until the pH was neutral, and then measured using a CE Model 440 Elemental Analyzer. The C/N ratio was derived from the ratio of TOC and TN. *n*-Alkanes were extracted based on methods described previously (Kawamura et al. 2003) in G-MOL lab of the University of Glasgow. Briefly, 2-10 g of freeze-dried, homogenized sediment were transferred to a test tube and hydrolyzed with 15 ml of 0.3 M KOH dissolved in 95:5 methanol/dichloromethane-extracted water. The samples were then hydrolyzed and centrifuged and the supernatant and pipetted into a round-bottomed flask. The sediment was then extracted three times with 10 ml dichloromethane/methanol (3:1) using ultrasonication. The extracts were combined and concentrated, using a rotary evaporator, under vacuum and then separated into neutral and acidic fractions using the methods of Kawamura (1995). The neutral fraction was further separated using silica gel column chromatography to get *n*-alkane fraction. Dried *n*-alkane fraction was redissolved in hexane and analyzed using a gas chromatograph (GC; Shimadzu

2010) with a flame ionization detector (FID) and hydrogen as carrier gas at constant pressure (190 kPa). Separation of the different compounds was achieved using an identical column (length: 60 m, diameter: 0.25 mm, film thickness: 0.25 μ m, coating: 100 % dimethyl-polysiloxane). The gas chromatograph temperature program was set to increase from 50 -120 $^{\circ}$ C at 30 $^{\circ}$ C min⁻¹, then 120 -310 $^{\circ}$ C at 5 $^{\circ}$ C min⁻¹, with a final isothermal time of 20 min at 300 $^{\circ}$ C. Compound identification was confirmed by GC/MS (Shimadzu OP2010-Plus Mass Spectrometer (MS) interfaced with a Shimadzu 2010 GC) based on retention times and mass spectra.

The *n*-alkane proxies (equation (1) from Poynter and Eglinton (1990); equation (2) from Marzi et al. (1993); and equation (3) from Ficken et al. (2000) were calculated as follows:

$$ACL = (19 \cdot C_{19} + 20 \cdot C_{20} + 21 \cdot C_{21} + \dots + 33 \cdot C_{33}) / (C_{19} + C_{20} + C_{21} + \dots + C_{33}) \quad (1)$$

$$CPI = 7/8 \cdot (C_{19} + C_{21} + C_{23} + \dots + C_{33}) / (C_{20} + C_{22} + C_{24} + \dots + C_{32}) \quad (2)$$

$$P_{aq} = (C_{23} + C_{25}) / (C_{23} + C_{25} + C_{29} + C_{31}) \quad (3)$$

where C_i is the concentration of *n*-alkane of *i* number of carbon.

Age model

The chronology of core GSA07-1 used in this study mainly consists of 19 dates from Zhao et al. (2010) and 6 new dates (Table 1). All ¹⁴C dates were measured in the AMS Dating Laboratory of Beijing University and are based on the leaves of terrestrial plants. The ages were calibrated to calendar years before present (AD 1950) using the

174 program CALIB Rev. 5.0.1 with the IntCal04 calibration data set (Reimer et al. 2004).

175 The depths of characteristic laminations in cores GSA07-1 and core GSB07-1 are
176 consistent. Therefore, the chronology of core GSB07-1 was calibrated based on the
177 corresponding depths in GSA07-1 (Table 1). The chronology indicates that the age of
178 core GSB07-1 spans the past 5720 years (Fig. 2). The average accumulation rate
179 based on the age-depth model is about 1.85 mm a⁻¹.

181 Results

183 *n*-Alkane distributions and P_{aq} variations in modern vegetation

186 The P_{aq} index has been proposed as an indicator of the relative contributions of
187 *n*-alkanes from submerged/floating aquatic plants versus those from emergent and
188 terrestrial plants in the lake. Generally, P_{aq} < 0.1 corresponds to terrestrial plants,
189 0.1-0.4 to emergent macrophytes, and 0.4-1.0 to submerged/floating macrophytes
190 (Ficken et al. 2000). In this study, average P_{aq} values and *n*-alkane molecular
191 distribution patterns vary considerably in the three types of plant material (terrestrial,
192 and emergent and submerged macrophytes: Fig. 3a-c). Terrestrial plants (Fig. 3a),
193 which have a lower average P_{aq} value (0.18), are dominated by the *n*-C₃₁ homologue.
194 Emergent macrophytes (Fig. 3b) growing in the near-shore environment are mainly
195 dominated by the *n*-C₂₇ homologue and have a higher P_{aq} value (0.65). In contrast,
196 *n*-C₂₃ is the dominant homologue in the submerged macrophytes (Fig. 3c) with a
197 secondary peak at *n*-C₂₅. The average P_{aq} value of submerged macrophytes is 0.93. In

addition, a bimodal *n*-alkane distribution pattern with high abundances at *n*-C₂₃ and
n-C₃₁ is observed in the surface sediments of Tianchi Lake which have an average P_{aq}
 value of 0.51 (Fig. 3d), indicating a specific mixture of inputs from terrestrial plants
 and submerged macrophytes. The distribution pattern for the surface soil has an
 overwhelming preponderance of the *n*-C₃₁ homologue, and the average P_{aq} value of
 the surface soils is 0.25 (Fig. 3e).

n-Alkane proxies and C/N ratios in the down-core sediments

Time series of the various sedimentary parameters are illustrated in Fig. 4. The
 records span the last 5.7 ka BP. P_{aq} (Fig. 4a) ranges from 0.32 to 0.78 with a mean of
 0.56. The average P_{aq} value is 0.46 during 5.7-3.2 ka BP, and 0.65 from 3.2 ka BP to
 the present. It is noteworthy that prior 3.2 ka BP most of the P_{aq} values are less than
 0.52, while subsequently they are greater than 0.52. ACL ranges from 25 to 29 with a
 mean of 27.4 (Fig. 4b). The CPI values range from 1.7 to 8.8 with a mean of 5.2 over
 the last 5.7 ka BP (Fig. 4c). The C/N ratios (Fig. 4d) range from 9.5 to 26 with a mean
 of 15. The ACL, CPI, and C/N ratios exhibit similar patterns of variation, and they all
 exhibit an obvious shift at 3.2 ka BP, as do the P_{aq} values. The threshold values of
 ACL, CPI, and C/N ratios are almost the same as their average values.

Discussion

1 220 Sources of organic matter to the lake

2
3 221

4
5
6 222 The organic component of lake sediments represents a pool of organic matter derived

7
8
9 223 from the decomposing detritus of aquatic plants growing in the littoral and marginal

10
11
12 224 zone of the lake and from terrestrial plants growing in the catchment (Meyers and

13
14 225 Ishiwatari 1993; Meyers 1997). Lacustrine sediment *n*-alkanes often have multiple

15
16
17 226 sources, including terrestrial plants, aquatic macrophytes and lower organisms.

18
19
20 227 Generally, *n*-alkane distributions of terrestrial and emergent plants tend to exhibit

21
22 228 high proportions of the *n*-C₃₁ homologue (Rielley et al. 1991; Ficken et al. 2000;

23
24
25 229 Sachse et al. 2006), whereas those of submerged and floating plants are generally

26
27
28 230 dominated by *n*-C₂₃ and *n*-C₂₅ homologues (Ficken et al. 2000; Gao et al. 2011; Seki

29
30
31 231 et al. 2012). Therefore, *n*-alkanes can be used to identify local and regional sources of

32
33
34 232 organic matter. However, recent studies have indicated that aquatic plants also make a

35
36
37 233 large contribution to the long chain *n*-alkanes in lake sediments (Aichner et al. 2010;

38
39
40 234 Liu et al. 2015; Liu and Liu 2016). For example, Liu et al. (2015) found that the long

41
42 235 chain *n*-alkanes produced by submerged plants in Qinghai Lake had a significant

43
44
45 236 influence on *n*-C₂₇ and *n*-C₂₉ alkanes in sediments. Even for the same submerged

46
47
48 237 plant (*Potamogeton* sp.) from 16 Tibetan Plateau lakes, the distribution patterns of all

49
50
51 238 the *n*-alkane homologs show obvious differences (Liu and Liu 2016). It is thus

52
53
54 239 necessary to make a distinction between the various sources that contribute to the

55
56
57 240 organic matter in given study area. At present, the two types of submerged

58
59 241 macrophytes (*Potamogeton* and *Chara*) in Tianchi Lake are dominated by mid-chain

60
61
62
63
64
65

n-alkanes (*n*-C₂₃ and *n*-C₂₅) (Fig. 3c). The average P_{aq} value is as high as 0.93. There is no evidence that they exhibit relatively high abundance of long chain *n*-alkanes as Liu and Liu (2016) described. The unimodal distribution pattern with the maxima at *n*-C₃₁ alkanes and relatively low P_{aq} values of modern terrestrial plants (Fig. 3a) and surface soils (Fig. 3e) in Tianchi Lake, suggest again that *n*-C₃₁ alkanes can be traced to terrestrial plant inputs and not to lake macrophytes. In addition, a bimodal molecular distribution pattern with major peaks at the *n*-C₂₃ and *n*-C₃₁ homologues in the surface lake sediments (Fig. 3d) probably represents a combination of inputs from submerged macrophytes (Fig. 3c) and terrestrial plants (Fig. 3a)/emergent (Fig. 3b). Our observations are consistent with those of previous studies (Cranwell 1984; Ficken et al. 2000; Gao et al. 2011; Street et al. 2013), which indicate that P_{aq} can be used to reflect the contribution from submerged macrophytes.

Interpretation of *n*-alkane indices

It has been demonstrated that the abundance of submerged macrophytes in lake is affected by irradiance and the littoral slope (Hudon 1997; Hudon et al. 2000; Cheruvilil and Soranno 2008). Thus, lake level has the potential to constrain the spatial distribution of submerged macrophytes via both a reduction in light intensity (Duarte and Kalf 1986; Middelboe and Markager 1997) and a change in the spatial extent of the littoral habitat (Hudon 1997). Hence, changes in the relative inputs of submerged macrophytes can potentially be ascribed to fluctuations in lake level. Most

of the submerged macrophytes in Tianchi Lake are distributed in a shallow area close to the shoreline and very few floating macrophytes can be observed (Fig. 1d). *Potamogeton* and *Chara* are the two dominant submerged species, which grow in a narrow zone down to a depth of ~1.2 m. A bathymetric survey of Tianchi Lake (Fig. 1b) reveals that the shoreline forms a narrow shelf from a depth of 0.5 m down to 2.8 m, followed by a steep slope that causes a decrease in the occurrence of submerged macrophytes. Assuming that the basic bathymetry of the basin has remained similar through time, the reductions in lake level would result in a relatively larger shelf area, which would produce an expansion of the shallow-water habitat for submerged macrophytes. Accordingly, the lower P_{aq} values in Tianchi Lake could be interpreted as reflecting less abundance of submerged macrophytes and the raising of lake level. On the other hand, the contribution from terrestrial plants can also exert an influence on P_{aq} values since the P_{aq} index is a proxy for evaluating the contribution of *n*-alkanes from submerged/floating aquatic plants relative to emergent and terrestrial plants (Ficken et al. 2000). During intervals of high rainfall and lake level, an increased contribution of terrestrial plant material delivered by increased catchment rain and runoff could lower P_{aq} values, and vice versa. This coincides with the findings of Liu and Liu (2016), which indicated a negative relationship between the P_{aq} value of surface lake sediments and the water level of Qinghai Lake.

As an important parameter of *n*-alkanes, the climate implications of ACL have been discussed a lot in the literature, but there is no unified agreement as to their interpretation because ACL often appears highly specific to regional or local

conditions (Ling et al. 2017). Furthermore, ACL can not be used to reconstruct
 temperature or precipitation change if the plant species or sedimentary environment in
 the catchment area underwent considerable change (in parallel with or forced by
 climatic variation) (Pu et al. 2010). CPI is another *n*-alkane index, which has been
 widely accepted as an indicator for terrestrial sources of sedimentary organic matter.
 Terrestrial plants have abundant long-chain *n*-alkanes, and show distinct odd-even
 predominance, thus their CPI is always greater than 5. On the contrary, CPI values of
 the aquatic plants and planktonic bacteria are considerably lower than those usually
 reported for terrestrial plant sourced *n*-alkanes (Cranwell 1987).

Reconstruction of the lake-level evolution

n-Alkane based records and C/N ratios from Tianchi Lake are presented in Fig. 4.
 Overall, there is an obvious shift at ~3.2 ka BP among the various proxies. During
 5.7-3.2 ka BP, the ACL (Fig. 4b) and CPI (Fig. 4c) proxies show relatively high
 values in the core. CPI values almost greater than 5 and ACL values range from 27 to
 29, likely indicate a predominance of terrestrial plant inputs to the lake basin. The
 results are supported by the higher C/N ratios (mean >15, with occasional values up to
 26) (Fig. 4d) in this phase since the C/N ratios from terrestrial plants and emergent
 macrophytes can be as high as 20 (Lamb et al. 2004). On the other hand, relatively
 lower P_{aq} values (0.32 - 0.56) (Fig. 4a) and a contrary changing trend of P_{aq} with ACL,
 CPI, C/N ratios, suggest a recession of the submerged macrophytes growing in

1 308 Tianchi Lake. Based on interpretations discussed above, less abundance of submerged
2
3 309 macrophytes input and more abundance of terrestrial plants input to the sediments are
4
5
6 310 likely a response to relatively high lake levels during this phase in Tianchi Lake.
7

8
9 311 We interpret the increase in average P_{aq} values (0.51-0.78) and a decrease in ACL
10
11 312 (25-27) and CPI (1.6-5.4) after 3.2 ka BP (Fig. 4a) as corresponding to an increase in
12
13
14 313 the proportion of submerged and floating-leaved macrophytes, and a decrease in
15
16
17 314 terrestrial inputs. Furthermore, the C/N ratios are generally low (<15) during this
18
19
20 315 interval. In view of the absence of floating-leaved macrophytes in Tianchi Lake,
21
22
23 316 based on our field observations, the increasing contribution from submerged
24
25
26 317 macrophytes accordingly indicates a gradually falling lake level from 3.2 ka BP.
27

28 318 The variations in lake level inferred by the *n*-alkanes record is also supported by a
29
30
31 319 shift in pollen assemblages from Tianchi Lake, which indicate that closed canopy
32
33
34 320 forest was replaced by an open landscape at around 3.0 ka BP (Zhao et al. 2010).
35

36 321 Another high-resolution pollen record from the Dadiwan peatland (Fig. 1a), 50 km
37
38
39 322 southwest of Tianchi Lake on the Loess Plateau, also reveals a significant decrease in
40
41
42 323 tree pollen frequencies at around 3.0 ka BP (An et al. 2003).
43
44
45 324

46
47 325 Asynchronous hydroclimatic variability
48
49
50 326

51
52
53 327 The P_{aq} record from Tianchi Lake reveals a transition from higher lake levels to lower
54
55
56 328 lake levels after 3.2 ka BP, and thus wetter conditions during 5.7-3.2 ka BP and drier
57
58
59 329 conditions after 3.2 ka BP (Fig. 5d). This accords with other paleoclimatic records
60
61
62
63
64
65

from the nearby Chinese Loess Plateau (Lu et al. 2013; Chen et al. 2015a; Liu et al. 2015; Rao et al. 2016). The pollen-based annual precipitation reconstruction from Tianchi Lake suggests a rapid precipitation decrease since ~3.3 ka BP (Fig. 5e; Chen et al. 2015a). Another pollen-based annual precipitation reconstruction from nearby Gonghai Lake (Fig. 5f) reveals a humid interval around 8-3 ka BP (Chen et al. 2015a). A recent study of palaeosol development as an indicator of the strength of the EASM (Wang et al. 2014) suggests a wet interval during 8.6-3.2 ka BP in the Chinese Loess Plateau. In addition, a TOC record from the Dadiwan peat profile also revealed a similar pattern of wet and dry episodes as at Tianchi Lake (Zhou et al. 1996; Huang et al. 2013). This evidence supports the contention that a moist climate was a widespread phenomenon on the Chinese Loess Plateau during the mid-Holocene. It is in accord with the gradually decreasing solar insolation (Fig. 5g). However, the paleohydrological conditions reconstructed from Dajiuhu peatland (Fig. 5c) in the middle reaches of the Yangtze River of central China are in contrast with these previous paleoclimatic records. Changes in the aerobic bacteria-derived hopanoid flux in Dajiuhu peatland (Fig. 5c) imply relatively arid conditions from 7.0-3.0 ka BP and relatively wet conditions from 3.0-1.0 ka BP (Xie et al. 2013; Huang et al. 2013; He et al. 2015). Another late-Holocene paleohydrological reconstruction based on sediment grain-size and *n*-alkane data from Longgan Lake in the middle and lower reaches of the Yangtze River (Xue et al. 2017), indicated drought conditions from 4 to 2.7 ka BP and a humid interval from 2.7 to 1.2 ka BP. In addition, the studies on the $\delta^{18}\text{O}$ (Fig. 5a) and the flux of soil-derived magnetic minerals preserved (Fig. 5b) in stalagmite

1 352 HS4 from Heshang cave in central China also revealed a relatively arid interval from
2
3 353 6.7 to 3.4 ka BP (Hu et al. 2008; Zhu et al. 2017). Therefore, it seems that mid-late
4
5
6 354 Holocene paleohydrological evolution was asynchronous in the middle reaches of the
7
8
9 355 Yangtze River of central China and in the Yellow River region of north China.

10
11 356 Tianchi Lake is located in the ‘far-field’ northwestern marginal region of the
12
13
14 357 EASM, whereas the Dajiuhu peatland (Fig. 1a) is located in the ‘core’ monsoonal area
15
16
17 358 of the EASM (Qian et al. 2007). Summer rainfall is the predominant contributor to the
18
19
20 359 annual precipitation at both sites (Gao and Xie 2014). The northwards advance of the
21
22
23 360 rainfall front resulting from an enhanced EASM intensity could result in increased
24
25
26 361 precipitation in the marginal region of the EASM but decreased precipitation in the
27
28
29 362 core monsoonal area of EASM (Ding et al. 2008; Rao et al. 2016). The occurrence of
30
31 363 this contrasting spatial pattern of moisture conditions, with more frequent droughts in
32
33
34 364 north China and more frequent floods in the mid-low Yangtze River valley during
35
36
37 365 summer, has also been observed during the last few decades (Gemmer et al. 2004;
38
39 366 Qian and Lin 2005; Zhai et al. 2005). It has been designated the “northern China
40
41
42 367 drought and southern China flood” precipitation pattern (Zhou et al. 2009), and is also
43
44
45 368 evident on millennial and centennial time scales (Chen et al. 2015b).

46
47 369 Previous workers have analyzed the main factors responsible for the
48
49
50 370 asynchronous pattern of hydroclimatic variability between the marginal and core
51
52
53 371 monsoonal area of EASM in China. For example, He et al. (2014) suggested that
54
55
56 372 terrestrial temperature-induced evaporation changes and the extent of the Asian
57
58
59 373 monsoonal front could potentially explain the out-of-phase pattern of hydrological

changes during the mid-Holocene. Chen et al. (2015a) emphasized that insolation forcing, especially the tropical ocean conditions might be responsible for the abrupt decline at 3.3 ka. Chen et al. (2015b) concluded that ENSO is one of the most important factors affecting the precipitation of monsoonal northern and central China on the centennial scale. Rao et al. (2016) emphasized the important influence of the west-east thermal gradient in the equatorial Pacific on the climate of monsoonal China. Zhu et al. (2017) concluded that a mid-Holocene reduction in ENSO intensity was related to a decrease in storm frequency in the middle reaches of Yangtze River between 6.7 and 3.4 ka BP. Finally, it is likely that the sea surface temperature (SST) anomaly in the equatorial Pacific during the mid-Holocene probably played a key role in facilitating the influence of ENSO on the asynchronous pattern of precipitation in the marginal and core monsoonal area of the EASM in China.

Conclusions

We have used the record of *n*-alkanes extracted from a lacustrine sediment core from Tianchi Lake on the Chinese Loess Plateau to reconstruct lake-level variations during the past 5.7 ka BP. P_{aq} values and C/N ratios through the sequence in general exhibit a gradually increasing trend through the past 5.7 ka BP, indicating an increasing (and more variable) abundance of submerged macrophytes in response to a falling lake level. Terrestrial plants dominated the record before 3.2 ka BP, and subsequently there was a shift to the dominance of submerged macrophytes. The predominance of

terrestrial plants agree with higher ACL, higher CPI, and lower P_{aq} values from 5.7-3.2 ka BP, whereas the dominance of submerged macrophytes resulted in lower ACL, lower CPI, and higher P_{aq} values after 3.2 ka BP. These changes indicate a relatively humid interval during 5.7-3.2 ka BP and a drier but more variable interval after 3.2 ka BP on the Chinese Loess Plateau. These findings are consistent with previous paleoclimatic reconstructions for the Loess Plateau which indicate a humid mid-Holocene. However, they are in disagreement with paleoclimatic records from central China, which indicate an arid mid-Holocene. Overall, this spatial pattern indicates that an enhanced intensity of monsoon rainfall delivered by the EASM during the mid-Holocene was an important factor in affecting paleohydrological changes in the region.

Acknowledgments

We thank Dr.Christopher Gallacher and Dr. Heiko Moossen for their training and help with laboratory analyses. This research was supported by grants from the National Science Foundation of China (NSFC Grants 41761044 and 41771208). We thank the China Scholarship Council (CSC) for funding a 20-month visit (File no. 2009618032) by Huiling Sun to work with Dr. James Bendle (now at the University of Birmingham) as a joint Ph.D. student (Lanzhou-Glasgow) at the G-MOL laboratory in Glasgow.

References

- An CB, Feng ZD, Tang LY (2003) Evidence of a humid mid-Holocene in the western part of Chinese Loess Plateau. *Chin Sci Bull* 48: 2472-2479
- Chen FH, Yu ZC, Yang ML, Ito E, Wang SM, Madsen DB, Huang XZ, Zhao Y, Sato T, Birks HJB, Boomer I, Chen JH, An CB, Wuennemann B (2008) Holocene moisture evolution in arid central Asia and its out-of-phase relationship with Asian monsoon history. *Quat Sci Rev* 27: 351-364
- Chen FH, Xu QH, Chen JH, Birks HJB, Liu JB, Zhang SR, Jin LY, An CB, Telford RJ, Cao XY, Wang ZL, Zhang XJ, Selvaraj K, Lu HY, Li YC, Zheng Z, Wang HP, Zhou AF, Dong GH, Zhang JW, Huang XZ, Bloemendal J, Rao ZG (2015a) East Asian summer monsoon precipitation variability since the last deglaciation. *Sci Rep* 5: 11186
- Chen JH, Chen FH, Feng S, Huang W, Liu JB, Zhou AF (2015b) Hydroclimatic changes in China and surroundings during the Medieval Climate Anomaly and Little Ice Age: spatial patterns and possible mechanisms. *Quat Sci Rev* 107: 98-111
- Cheruvilil KS, Soranno PA (2008) Relationships between lake macrophyte cover and lake and landscape features. *Aquat Bot* 88: 219-227
- Clift PD, Plumb RA (2008) The Asian monsoon: causes, history and effects. Cambridge University Press, Cambridge
- Cranwell PA (1984) Lipid geochemistry of sediments from Upton Broad, a small productive lake. *Org Geochem* 7: 25-37
- Ding YH, Wang ZY, Sun Y (2008) Inter-decadal variation of the summer precipitation in East China and its association with decreasing Asian summer monsoon. Part I: Observed

441 evidences. *Int J Climatol* 28: 1139-1161
 442 Dong GH, Yang Y, Zhao Y, Zhou AF, Zhang XJ, Li XB, Chen FH (2012) Human settlement
 443 and human-environment interactions during the historical period in Zhuanglang County,
 444 western Loess Plateau, China. *Quat Int* 281: 78-83
 445 Duarte CM, Kalf J (1986) Littoral slope as a predictor of the maximum biomass of submerged
 446 macrophyte communities. *Limnol Oceanogr* 31: 1072-1080
 447 Ficken KJ, Li B, Swain DL, Eglinton G (2000) An *n*-alkane proxy for the sedimentary input
 448 of submerged/floating freshwater aquatic macrophytes. *Org Geochem* 31: 745-749
 449 Gao L, Hou JZ, Toney J, MacDonald DL, Huang YS (2011) Mathematical modeling of the
 450 aquatic macrophyte inputs of mid-chain *n*-alkyl lipids to lake sediments: implications for
 451 interpreting compound specific hydrogen isotopic records. *Geochim Cosmochim Acta* 75:
 452 3781-3791
 453 Gao T, Xie LA (2014) Study on progress of the trends and physical causes of extreme
 454 precipitation in China during the last 50 years. *Adv Earth Sci* 29: 577-589
 455 Gemmer M, Becker S, Jiang T (2004) Observed monthly precipitation trends in China
 456 1951-2002. *Theor Appl Clim* 77: 39-45
 457 He YX, Zheng YW, Pan AD, Zhao C, Sun YY, Song M, Zheng Z, Liu ZH (2014)
 458 Biomarker-based reconstructions of Holocene lake-level changes at Lake Gahai on the
 459 northeastern Tibetan Plateau. *The Holocene* 24: 405-412
 460 He YX, Zhao C, Zheng Z, Liu ZH, Wang N, Li J, Cheddadi R (2015) Peatland evolution and
 461 associated environmental changes in central China over the past 40,000 years. *Quat Res* 84:
 462 255-261

463 Huang XY, Xue JT, Wang XX, Meyers PA, Huang JH, Xie SC (2013) Paleoclimate influence
 464 on early diagenesis of plant triterpenes in the Dajiuhu peatland, central China. *Geochim*
 465 *Cosmochim Acta* 123: 106-119
 466 Hudon C (1997) Impact of water level fluctuations on St. Lawrence River aquatic vegetation.
 467 *Can J Fish Aquat Sci* 54: 2853-2865
 468 Hudon C, Lalonde S, Gagnon P (2000) Ranking the effects of site exposure, plant growth
 469 form, water depth, and transparency on aquatic plant biomass. *Can J Fish Aquat Sci* 57: 31-42
 470 Kawamura K (1995) Land-derived lipid class compounds in the deep-sea sediments and
 471 marine aerosols from North Pacific. In: *Biogeochemical Processes and Ocean Flux in the*
 472 *Western Pacific*. Terra Scientific Publishing Company, Tokyo, pp 31-51
 473 Kawamura K, Ishimura Y, Yamazaki K (2003) Four years' observations of terrestrial lipid
 474 class compounds in marine aerosols from the western North Pacific. *Global Biogeochem Cy*
 475 17: 3-1-3-19
 476 Lamb AL, Leng MJ, Mohammed MU, Lamb HF (2004) Holocene climate and vegetation
 477 change in the Main Ethiopian Rift Valley, inferred from the composition (C/N and $\delta^{13}\text{C}$) of
 478 lacustrine organic matter. *Quat Sci Rev* 23: 881-891
 479 Ling Y, Zheng MP, Sun Q, Dai XQ (2017) Last deglacial climatic variability in Tibetan
 480 Plateau as inferred from *n*-alkanes in a sediment core from Lake Zabuye. *Quat Int* 454: 15-24
 481 Liu FG, Feng ZD (2012) A dramatic climatic transition at ~4,000 cal. yr BP and its cultural
 482 responses in Chinese cultural domains. *The Holocene* 22: 1181-1197
 483 Liu H, Liu WG (2016) *n*-Alkane distributions and concentrations in algae, submerged plants
 484 and terrestrial plants from the Qinghai-Tibetan Plateau. *Org Geochem* 99: 10-22

485 Liu JB, Chen JH, Zhang XJ, Li Y, Rao ZG, Chen FH (2015) Holocene East Asian summer
 486 monsoon records in northern China and their inconsistency with Chinese stalagmite $\delta^{18}\text{O}$
 487 records. *Earth-Sci Rev* 148: 194-208
 488 Liu WG, Yang H, Wang HY, An ZS, Wang Z, Leng Q (2015) Carbon isotope composition of
 489 long chain leaf wax *n*-alkanes in lake sediments: A dual indicator of paleoenvironment in the
 490 Qinghai-Tibet Plateau. *Org Geochem* 83: 190-201
 491 Lu HY, Yi SW, Liu ZY, Mason JA, Jiang DB, Cheng J, Stevens T, Xu ZW, Zhang EL, Jin
 492 LY (2013) Variation of East Asian monsoon precipitation during the past 21 ky and potential
 493 CO_2 forcing. *Geology* 41: 1023-1026
 494 Marzi R, Torkelson BE, Olson RK (1993) A revised carbon preference index. *Org Geochem*
 495 20: 1303-1306
 496 Meyers PA (1997) Organic geochemical proxies of paleoceanographic, paleolimnologic, and
 497 paleoclimatic processes. *Org Geochem* 27: 213-250
 498 Meyers PA, Ishiwatari R (1993) Lacustrine organic geochemistry - an overview of indicators
 499 of organic matter sources and diagenesis in lake sediments. *Org Geochem* 20: 867-900
 500 Middelboe AL, Markager S (1997) Depth limits and minimum light requirements of
 501 freshwater macrophytes. *Freshw Biol* 37: 553-568
 502 Nichols JE, Booth RK, Jackson ST, Pendall EG, Huang YS (2006) Paleohydrologic
 503 reconstruction based on *n*-alkane distributions in ombrotrophic peat. *Org Geochem* 37:
 504 1505-1513
 505 Poynter J, Eglinton G (1990) Molecular composition of three sediments from hole 717c: The
 506 Bengal fan. In: *Proceedings of the Ocean Drilling Program: Scientific results*, 116: pp.

1 507 155-161

2

3 508 Pu, Y, Zhang HC, Lei GL, Chang FQ, Yang MS, Zhang WX, Lei YB, Yang LQ, Pang YZ

4

5

6 509 (2010) Climate variability recorded by *n*-alkanes of paleolake sediment in Qaidam Basin on

7

8

9 510 the northeast Tibetan Plateau in late MIS3. China Earth Sci: 53: 624-631 (In Chinese)

10

11 511 Qian W, Lin X (2005) Regional trends in recent precipitation indices in China. Meteorol

12

13 512 Atmos Phys 90: 193-207

14

15

16

17 513 Qian WH, Lin X, Zhu YF, Xu Y, Fu JL (2007) Climatic regime shift and decadal anomalous

18

19

20 514 events in China. Clim Change 84: 167-189

21

22

23 515 Qiang MR, Song L, Chen FH, Li MZ, Liu XX, Wang Q (2013) A 16 ka lake-level record

24

25 516 inferred from macrofossils in a sediment core from Genggahai Lake, northeastern

26

27

28 517 Qinghai-Tibetan Plateau (China). J Paleolimnol 49: 575-590

29

30

31 518 Rao ZG, Jia GD, Li YX, Chen JH, Xu QH, Chen FH (2016) Asynchronous evolution of the

32

33

34 519 isotopic composition and amount of precipitation in north China during the Holocene

35

36

37 520 revealed by a record of compound-specific carbon and hydrogen isotopes of long-chain

38

39

40 521 *n*-alkanes from an alpine lake. Earth Planet Sci Lett 446: 68-76

41

42 522 Reimer PJ, Baillie MGL, Bard E, Bayliss A, Beck JW, Bertrand CJH, Blackwell PG, Buck

43

44 523 CE, Burr GS, Cutler KB, Damon PE, Edwards RL, Fairbanks RG, Friedrich M, Guilderson

45

46

47 524 TP, Hogg AG, Hughen KA, Kromer B, McCormac FG, Manning SW, Ramsey CB, Reimer

48

49

50 525 RW, Remmele S, Southon JR, Stuiver M, Talamo S, Taylor FW, van der Plicht, J,

51

52

53 526 Weyhenmeyer CE, (2004) IntCal04 terrestrial radiocarbon age calibration, 0-26 cal kyr BP.

54

55

56 527 Radiocarbon 46: 1029-1058

57

58

59 528 Rielley G, Collier RJ, Jones DM, Eglinton G (1991) The biogeochemistry of Ellesmere Lake,

60

61

62

63

64

65

529 UK-I: source correlation of leaf wax inputs to the sedimentary lipid record. *Org Geochem* 17:
 530 901-912
 531 Sachse D, Radke J, Gleixner G (2006) δD values of individual *n*-alkanes from terrestrial
 532 plants along a climatic gradient - Implications for the sedimentary biomarker record. *Org*
 533 *Geochem* 37: 469-483
 534 Seki O, Harada N, Sato M, Kawamura K, Ijiri A, Nakatsuka T (2012) Assessment for
 535 paleoclimatic utility of terrestrial biomarker records in the Okhotsk Sea sediments. *Deep Sea*
 536 *Research Part II: Topical Studies in Oceanography* 61: 85-92
 537 Street JH, Anderson RS, Rosenbauer RJ, Paytan A (2013) *n*-Alkane evidence for the onset of
 538 wetter conditions in the Sierra Nevada, California (USA) at the mid-late Holocene transition,
 539 ~ 3.0 ka. *Quat Res* 79: 14-23
 540 Vogts A, Moossen H, Rommerskirchen F, Rullkötter J (2009) Distribution patterns and stable
 541 carbon isotopic composition of alkanes and alkan-1-ols from plant waxes of African rain
 542 forest and savanna C_3 species. *Org Geochem* 40: 1037-1054
 543 Wagner T, Falter CM (2002) Response of an aquatic macrophyte community to fluctuating
 544 water levels in an oligotrophic lake. *Lake Reservoir Manag* 18: 52-65
 545 Wang HP, Chen JH, Zhang XJ, Chen FH (2014) Palaeosol development in the Chinese Loess
 546 Plateau as an indicator of the strength of the East Asian summer monsoon: Evidence for a
 547 mid-Holocene maximum. *Quat Int* 334: 155-164
 548 Wang SW, Huang JB, Wen XY, Zhu JH (2008) Evidence and modeling study of droughts in
 549 China during 4-2 ka BP. *Chin Sci Bull* 53: 2215-2221
 550 Xie SC, Evershed RP, Huang XY, Zhu ZM, Pancost RD, Meyers PA, Gong LF, Hu CY,

551 Huang JH, Zhang SH, Gu YS, Zhu JY (2013) Concordant monsoon-driven postglacial
 552 hydrological changes in peat and stalagmite records and their impacts on prehistoric cultures
 553 in central China. *Geology* 41: 827-830
 554 Xue JT, Li JJ, Dang XY, Meyers PA, Huang XY (2017) Paleohydrological changes over the
 555 last 4,000 years in the middle and lower reaches of the Yangtze River: Evidence from particle
 556 size and *n*-alkanes from Longgan Lake. *The Holocene* 27: 1318-1324
 557 Zhai PM, Zhang XB, Wan H, Pan XH (2005) Trends in total precipitation and frequency of
 558 daily precipitation extremes over China. *J Climate* 18: 1096-1108
 559 Zhao Y, Chen FH, Zhou AF, Yu ZC, Zhang K (2010) Vegetation history, climate change and
 560 human activities over the last 6200 years on the Liupan Mountains in the southwestern Loess
 561 Plateau in central China. *Palaeogeogr Palaeoclimatol Palaeoecol* 293: 197-205
 562 Zhou TJ, Gong DY, Li J, Li B (2009) Detecting and understanding the multi-decadal
 563 variability of the East Asian Summer Monsoon-recent progress and state of affairs. *Meteorol*
 564 *Z* 18: 455-467
 565 Zhou WJ, Douglas JD, Stephen CP, Timothy AJ, Li XQ, Minze S, An ZS, Eiji M, Dong GR
 566 (1996) Variability of monsoon climate in East Asia at the end of the last glaciation. *Quat Res*
 567 46: 219-229
 568 Zhu ZM, Feinberg JM, Xie SC, Bourne MD, Huang CJ, Hu CY, Cheng H (2017) Holocene
 569 ENSO-related cyclic storms recorded by magnetic minerals in speleothems of central China.
 570 *Proc Natl Acad Sci* 114: 852-857

Figure captions

Fig. 1. (a) Location of Tianchi Lake in North China. Solid dots represent the study area and other study sites referenced in the text. The map shows the correlation coefficients between summer precipitation in China and summer monsoon intensity from 1951-2000 (Wang et al. 2008), (b) schematic representation of the bathymetry of Tianchi Lake (depths in m), (c) laminated structure of the sediment cores from Tianchi Lake, (d) photo of submerged macrophytes in the shallow area of Tianchi Lake

Fig. 2. Age-depth model for core GSB07-1 from Tianchi Lake

Fig. 3. Histogram of the molecular distributions of *n*-alkanes from (a) modern terrestrial plants, (b) modern emergent macrophytes, (c) modern submerged macrophytes, (d) surface lake sediments and (e) surface soils from around Tianchi Lake. Only odd carbon number distributions are shown for the *n*-alkanes

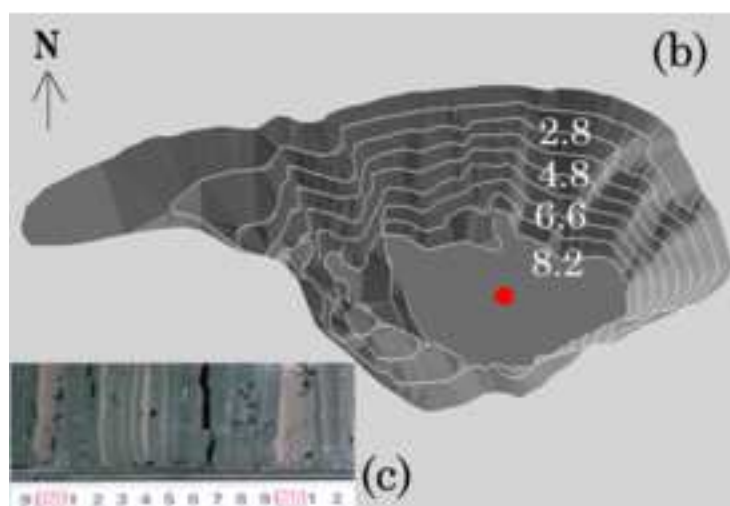
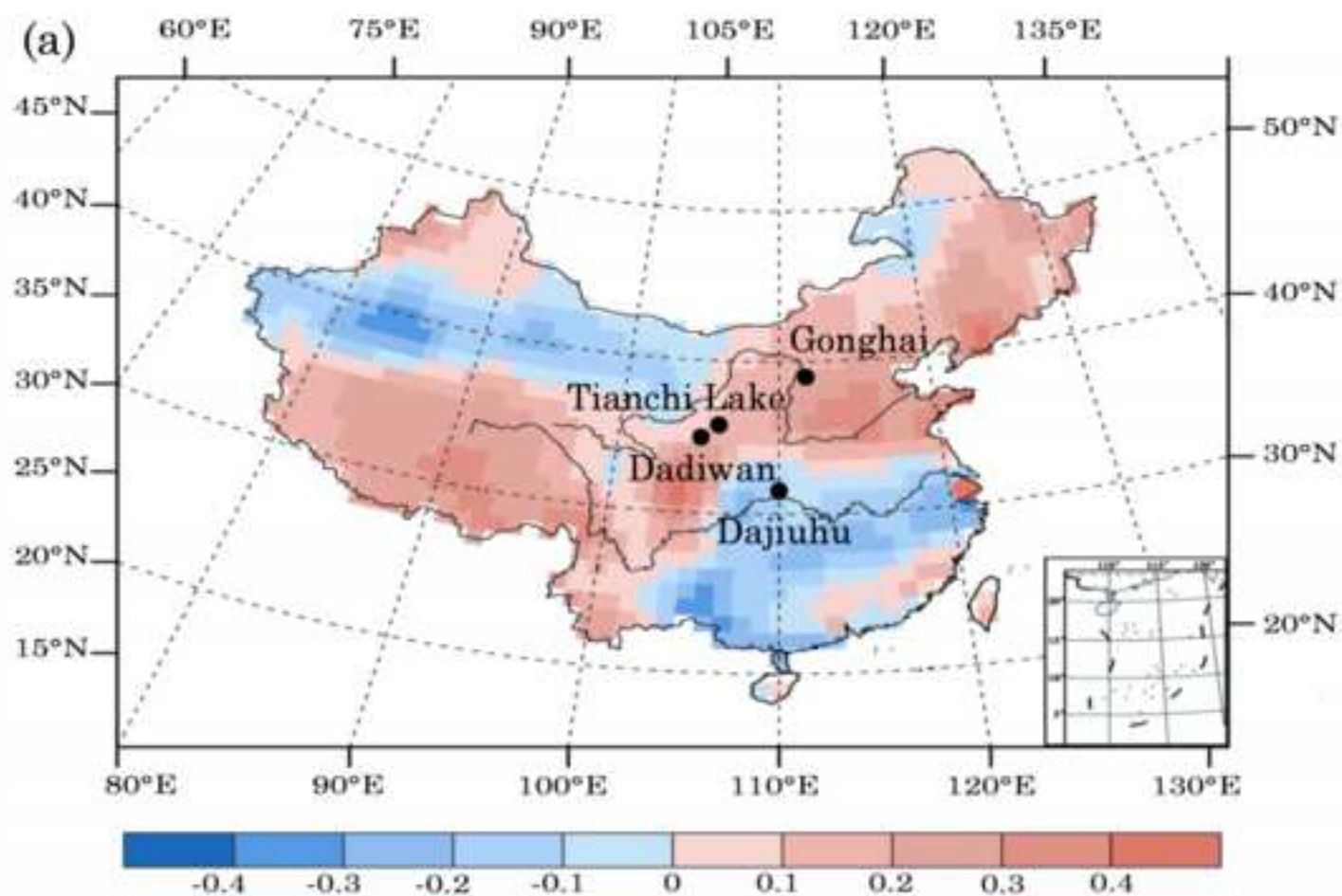
Fig. 4. Time series of sedimentary parameters for core GSB07-1 from Tianchi Lake over the past 5.7 ka BP. (a) P_{aq} values based-on *n*-alkanes, (b) *n*-alkane ACL, (c) *n*-alkane CPI, (d) C/N ratios

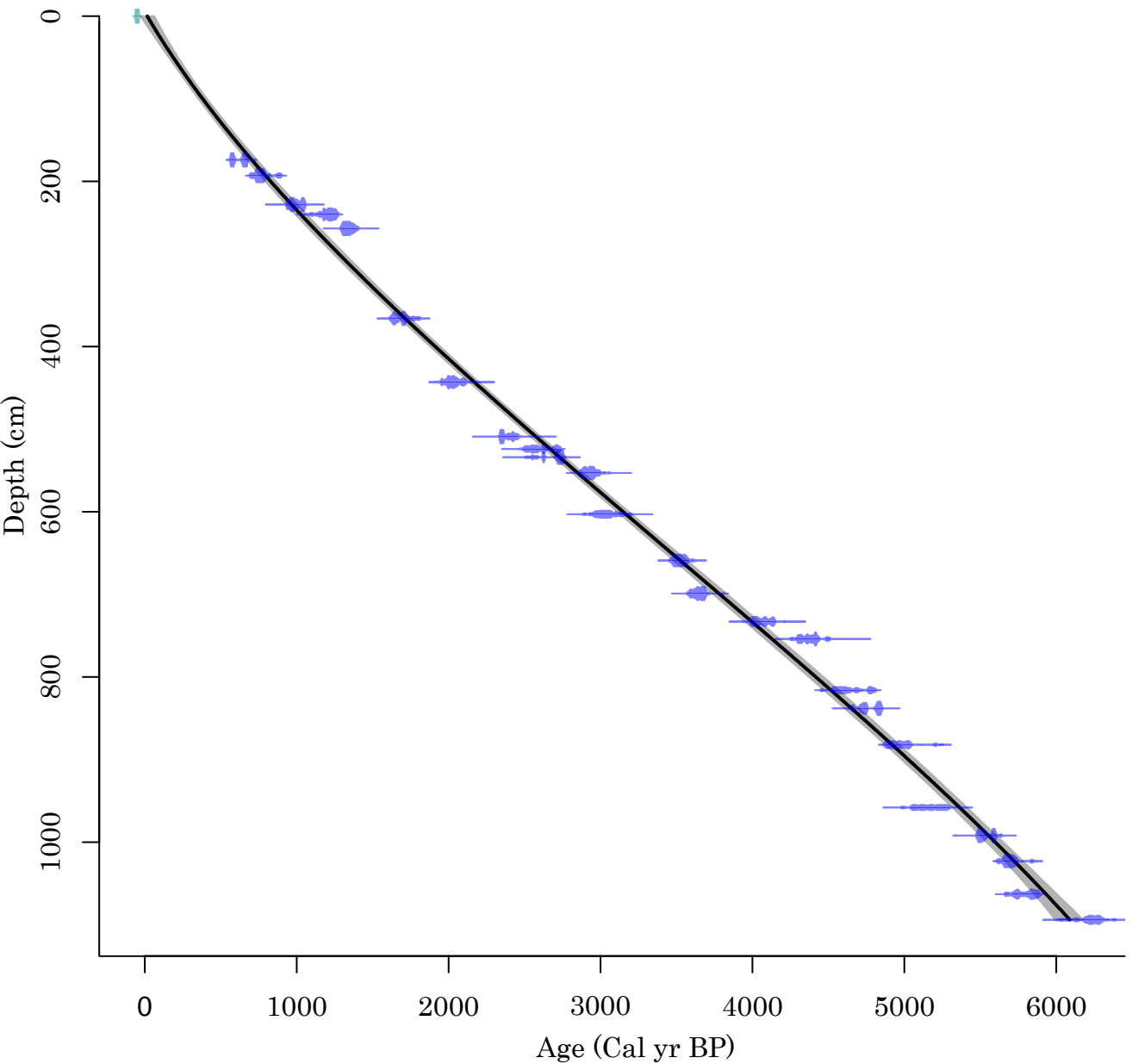
Fig. 5. Comparison of regional paleohydrological records. (a) Heshang cave speleothem $\delta^{18}O$ records (Hu et al. 2008), (b) the flux of soil-derived magnetic minerals ($IRM_{soft-flux}$) preserved in stalagmite HS4 (Zhu et al. 2017), (c) hopanoids

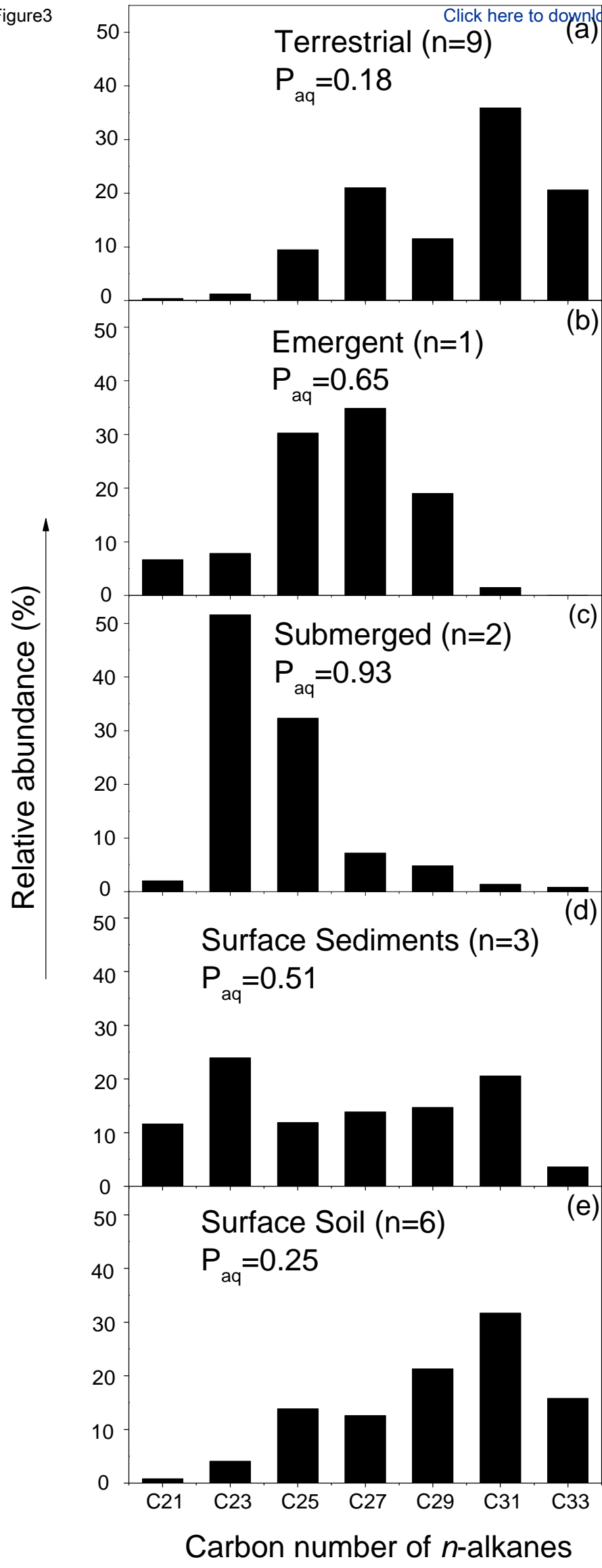
1 595 flux in Dajiuhu peatland (Xie et al. 2013), (d) P_{aq} values based-on *n*-alkanes in
2
3 596 Tianchi Lake, (e) pollen-based reconstruction of mean annual precipitation (MAP)
4
5
6 597 from Tianchi Lake (Chen et al. 2015a), (f) pollen-based reconstruction of mean annual
7
8
9 598 precipitation (MAP) from Gonghai Lake (Chen et al. 2015a), (g) July Insolation at
10
11
12 599 30 °N (Berger and Loutre 1991)
13
14 600
15
16
17 601
18
19
20 602
21
22
23 603
24
25
26 604
27
28 605
29
30
31 606
32
33
34 607
35
36
37 608
38
39 609
40
41
42 610
43
44
45 611
46
47
48 612
49
50
51 613
52
53
54 614
55
56 615
57
58
59 616
60
61
62
63
64
65

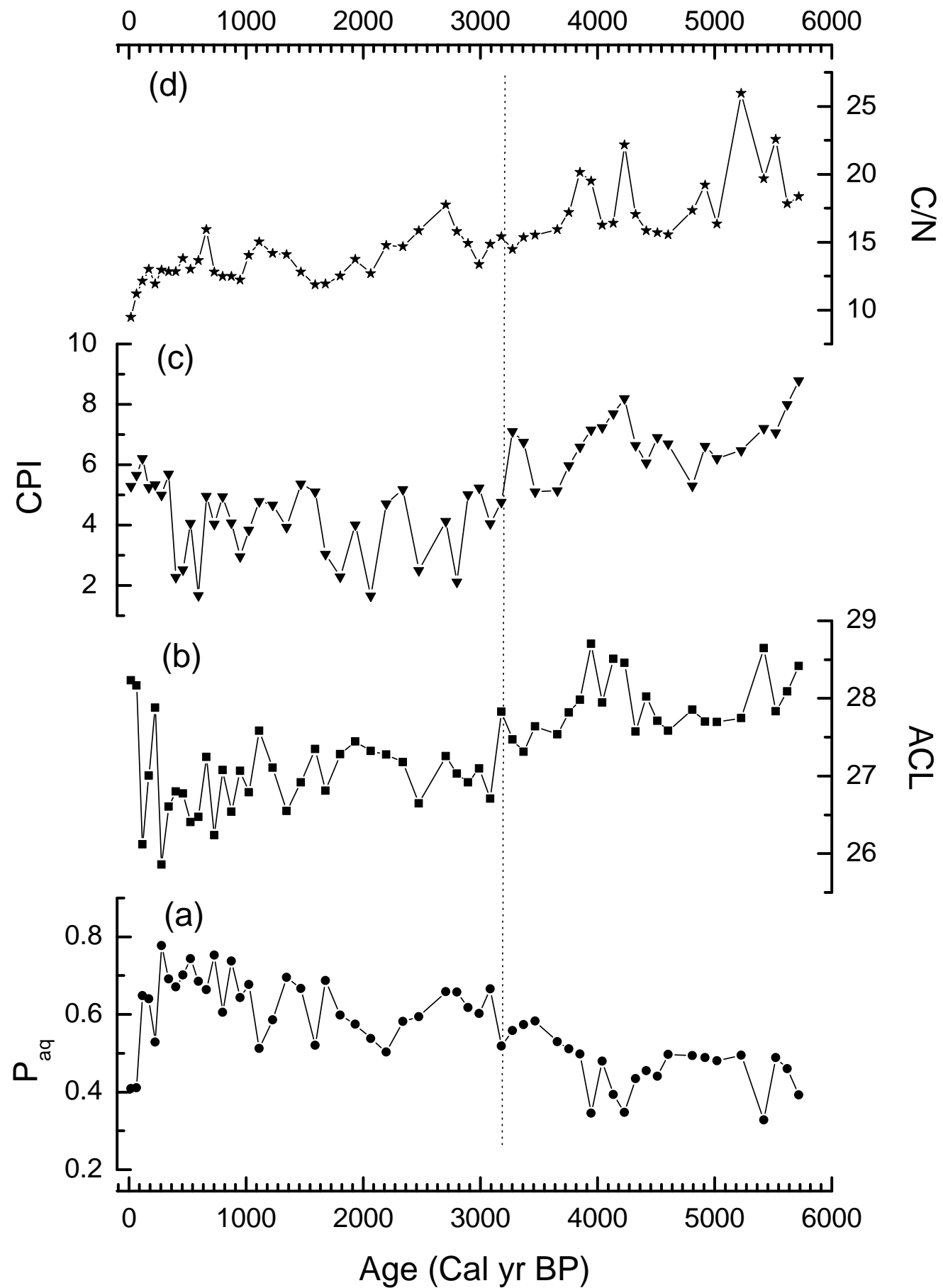
Table 1. AMS radiocarbon dates of core GSA07-1 in Tianchi Lake and the chronology of core GSB07-1 based on depth calibration with core GSA07-1

Core GSA07-1						Core GSB07-1	
Depth (cm)	Material dated	$\delta^{13}\text{C}$ (‰ VPDB)	^{14}C date (yr BP)	Error (\pm yr)	Calibrated age (Cal yr BP-2 σ range)	Calibrated depth (cm)	Calibrated age (Cal yr BP)
162	Tree leaves	-29.0	680	30	619 \pm 56	174	662 \pm 21
183	Tree leaves	-26.9	855	35	740 \pm 47	193	776 \pm 27
221	Tree leaves	-21.1	1080	35	963 \pm 35	228	1009 \pm 33
260	Tree leaves	-11.6	1255	30	1169 \pm 42	240	1088 \pm 23
302	Tree leaves	-18.7	1440	45	1378 \pm 37	257	1192 \pm 14
383	Tree leaves	-21.0	1775	30	1793 \pm 30	366	1768 \pm 58
436	Tree leaves	-24.3	2060	30	2089 \pm 42	443	2217 \pm 82
489	Tree leaves	-23.1	2355	30	2398 \pm 52	509	2633 \pm 37
510	Tree leaves	-17.6	2520	35	2537 \pm 49	526	2719 \pm 26
518	Tree leaves	-12.7	2585	40	2580 \pm 52	532	2754 \pm 25
554	Tree leaves	-26.3	2415	35	2789 \pm 51	545	2830 \pm 25
570	Tree leaves	-25.4	2830	30	2898 \pm 45	554	2891 \pm 30
600	Tree leaves	-16.6	2895	45	3097 \pm 51	593	3130 \pm 43
660	Tree leaves	-19.7	3300	30	3520 \pm 43	658	3538 \pm 38
701	Tree leaves	-30.3	3400	30	3793 \pm 36	700	3810 \pm 19
732	Tree leaves	-24.4	3720	35	4002 \pm 33	730	4012 \pm 28
751	Tree leaves	-20.2	3935	35	4149 \pm 45	754	4174 \pm 21
815	Tree leaves	-14.7	4100	40	4547 \pm 33	816	4540 \pm 29
848	Tree leaves	-19.5	4230	35	4726 \pm 33	838	4653 \pm 28
893	Tree leaves	-18.3	4400	40	4937 \pm 41	882	4899 \pm 33
966	Tree leaves	-16.3	4495	40	5277 \pm 33	957	5290 \pm 25
1014	Tree leaves	-25.6	4820	40	5513 \pm 32	992	5497 \pm 26
1049	Tree leaves	-27.1	4970	35	5689 \pm 34	1023	5673 \pm 33
1086	Tree leaves	-25.4	5030	35	5870 \pm 33		
1114	Tree leaves	-24.4	5440	70	6038 \pm 41		









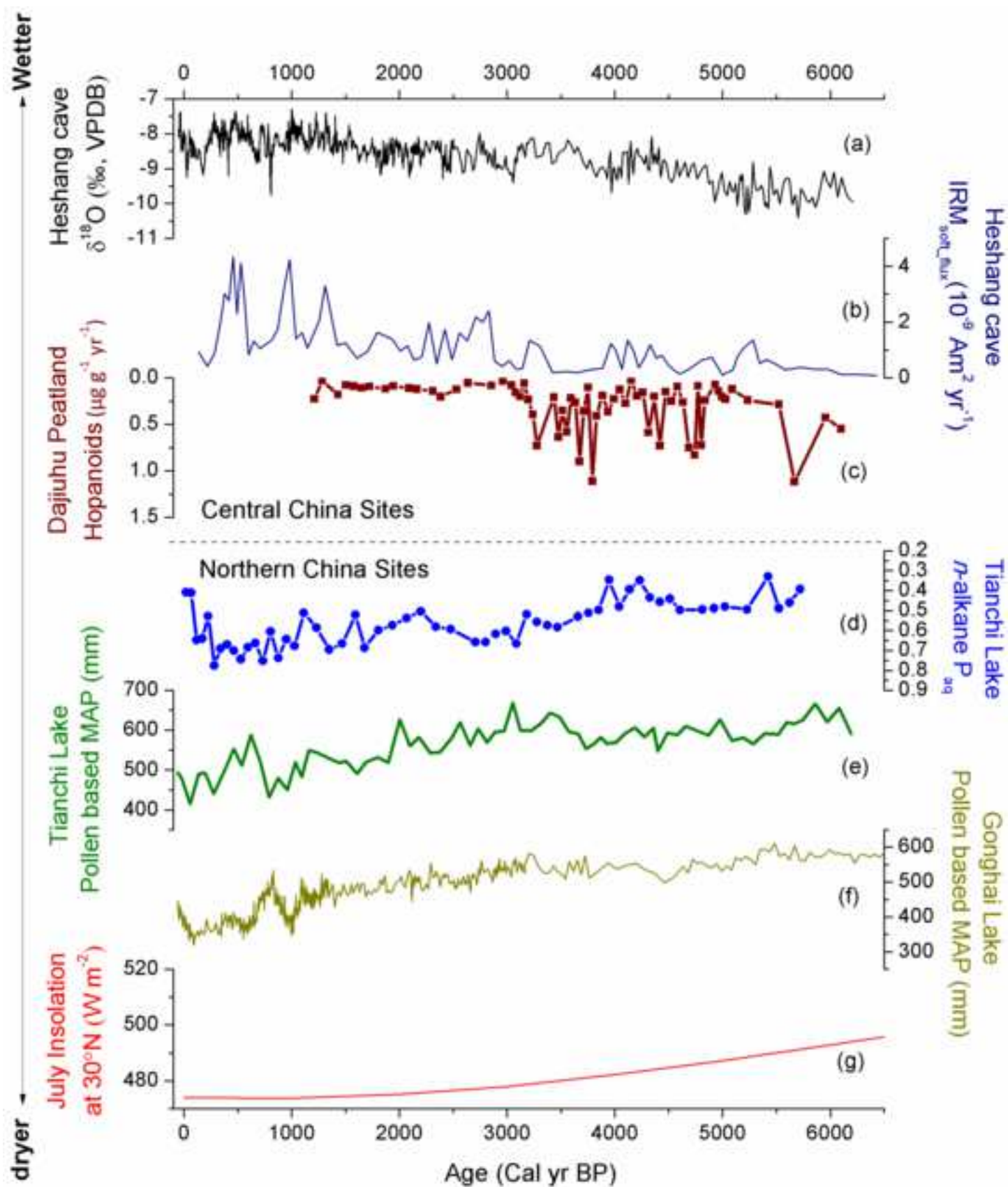


Table 1

Core GSA07-1						Core GSB07-1	
Depth (cm)	Material dated	δ13C (‰ VPDB)	14C date (yr BP)	Error (±yr)	Calibrated age (Cal yr BP-2σ range)	Calibrated depth (cm)	Calibrated age (Cal yr BP)
162	Tree leaves	-29.0	680	30	619±56	174	662±21
183	Tree leaves	-26.9	855	35	740±47	193	776±27
221	Tree leaves	-21.1	1080	35	963±35	228	1009±33
260	Tree leaves	-11.6	1255	30	1169±42	240	1088±23
302	Tree leaves	-18.7	1440	45	1378±37	257	1192±14
383	Tree leaves	-21.0	1775	30	1793±30	366	1768±58
436	Tree leaves	-24.3	2060	30	2089±42	443	2217±82
489	Tree leaves	-23.1	2355	30	2398±52	509	2633±37
510	Tree leaves	-17.6	2520	35	2537±49	526	2719±26
518	Tree leaves	-12.7	2585	40	2580±52	532	2754±25
554	Tree leaves	-26.3	2415	35	2789±51	545	2830±25
570	Tree leaves	-25.4	2830	30	2898±45	554	2891±30
600	Tree leaves	-16.6	2895	45	3097±51	593	3130±43
660	Tree leaves	-19.7	3300	30	3520±43	658	3538±38
701	Tree leaves	-30.3	3400	30	3793±36	700	3810±19
732	Tree leaves	-24.4	3720	35	4002±33	730	4012±28
751	Tree leaves	-20.2	3935	35	4149±45	754	4174±21
815	Tree leaves	-14.7	4100	40	4547±33	816	4540±29
848	Tree leaves	-19.5	4230	35	4726±33	838	4653±28
893	Tree leaves	-18.3	4400	40	4937±41	882	4899±33
966	Tree leaves	-16.3	4495	40	5277±33	957	5290±25
1014	Tree leaves	-25.6	4820	40	5513±32	992	5497±26
1049	Tree leaves	-27.1	4970	35	5689±34	1023	5673±33
1086	Tree leaves	-25.4	5030	35	5870±33	1060	5871±35
1114	Tree leaves	-24.4	5440	70	6038±41	1094	6078±58